Title

Human Vault Nanoparticle Targeted Delivery of Antiretroviral Drugs to Inhibit Human Immunodeficiency Virus Type 1 Infection

Journal

Bioconjugate Chemistry, 30(8)

ISSN

1043-1802

Authors

Fulcher, Jennifer A
Tamshen, Kyle
Wollenberg, Alexander L
et al.

Publication Date

2019-08-21

DOI

10.1021/acs.bioconjchem.9b00451

Peer reviewed

Published in final edited form as:

Bioconjug Chem. 2019 August 21; 30(8): 2216–2227. doi:10.1021/acs.bioconjchem.9b00451.

Human Vault Nanoparticle Targeted Delivery of Antiretroviral Drugs to Inhibit Human Immunodeficiency Virus Type 1 Infection

Jennifer A. Fulcher[†,Δ], **Kyle Tamshen**[‡,Δ], **Alexander L. Wollenberg**[‡,Δ], **Valerie A. Kickhoefer**[§], **Jan Mrazek**[†], **Julie Elliott**[¶], **F. Javier Ibarrondo**[†], **Peter A. Anton**[¶,£], **Leonard H. Rome**[§,¥], **Heather D. Maynard**[‡,¥,π], **Timothy Deming**[‡,¥,π], **Otto O. Yang**[†,£,*]

[†] Division of Infectious Diseases, Department of Medicine, David Geffen School of Medicine at UCLA, Los Angeles, CA, USA.

[‡] Department of Chemistry and Biochemistry, University of California, Los Angeles, CA, USA.

[§] Department of Biological Chemistry, David Geffen School of Medicine at UCLA, Los Angeles, CA, USA.

[¶] Vatche and Tamar Manoukian Division of Digestive Diseases, David Geffen School of Medicine at UCLA, Los Angeles, CA, USA.

[£] AIDS Healthcare Foundation, Los Angeles, CA, USA.

[¥] California NanoSystems Institute, University of California, Los Angeles, CA, USA.

[π] Department of Bioengineering, University of California, Los Angeles, CA, USA.

Abstract

"Vaults" are ubiquitously expressed endogenous ribonucleoprotein nanoparticles with potential utility for targeted drug delivery. Here we show that recombinant human vault nanoparticles are readily engulfed by certain key human peripheral blood mononuclear cells (PBMC), predominately dendritic cells, monocytes/macrophages, and activated T cells. As these cell types are the primary targets for human immunodeficiency virus type 1 (HIV-1) infection, we examined the utility of recombinant human vaults for targeted delivery of antiretroviral drugs. We chemically modified three different antiretroviral drugs, zidovudine, tenofovir, and elvitegravir, for direct conjugation to vaults. Tested in infection assays, drug-conjugated vaults inhibited HIV-1 infection of PBMC with equivalent activity to free drugs, indicating vault delivery and drug release in the cytoplasm of HIV-1-susceptible cells. The ability to deliver functional drugs via vault nanoparticle conjugates suggests their potential utility for targeted drug delivery against HIV-1.

Graphical Abstract

[*]Corresponding author: BSRB 173, 615 Charles E Young Drive South, Los Angeles, CA 90095, oyang@mednet.ucla.edu, Phone (310) 794-9491, Fax (310) 983-1067.
[Δ]These authors contributed equally

SUPPORTING INFORMATION AVAILABLE

Details regarding flow cytometry panels and antibodies as well as NMR and HRMS spectra for all chemicals is available in Supporting Information. This material is available free of charge via the internet at http://pubs.acs.org.

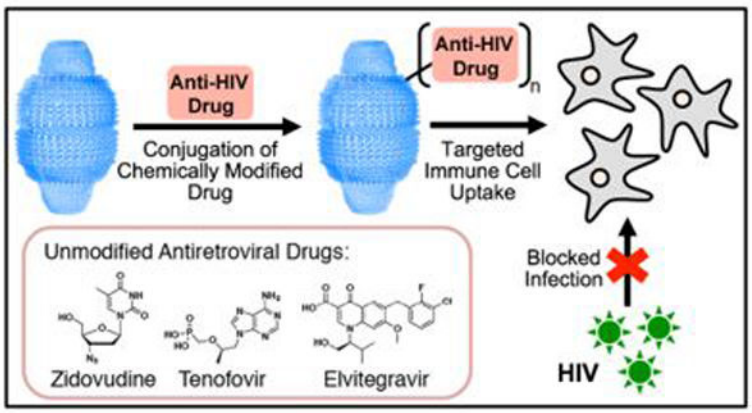

Keywords

Nanoparticle; drug conjugation; HIV-1; antiretroviral therapy; targeted drug delivery

INTRODUCTION

Targeted drug delivery can reduce drug toxicity while also increasing efficacy, and has been successfully utilized in cancer chemotherapy and immunotherapeutics.[1] Delivering drugs specifically to sites and/or cells involved in disease reduces systemic and increases local exposure, thereby achieving more specific treatment. The use of nanotechnology for targeted drug delivery in anti-HIV-1 microbicide development has been a promising focus because of the potential for these systems to aid in distribution, retention, and specific delivery of drugs at the sites of infection.

Despite highly effective antiretroviral therapy (ART) to treat HIV-1 infection, there is still no effective vaccine or cure. With about 1.8 million new HIV-1 infections in 2017[2], prevention strategies are key to HIV-1 eradication efforts. Pre-exposure prophylaxis (PrEP), which is the systemic administration of ART to HIV-1-uninfected persons to prevent infection, can be highly effective, but is highly dependent upon medication adherence and tissue penetration.[3–5] Additionally, systemically administered PrEP can have significant side effects and long-term toxicities. Thus, a major goal in HIV-1 prevention research is targeting drug delivery to improve efficacy while reducing potential toxicity.

Mucosal HIV-1 transmission accounts for the majority of transmission events. HIV-1 primarily infects activated $CD4^+$ T cells, the majority of which reside in the gastrointestinal mucosa.[6] Orally administered antiretroviral drugs vary greatly in penetration of rectal and vaginal mucosal tissues.[7] Thus, locally targeting therapy to the $CD4^+$ T cells in these vulnerable tissues could lead to better efficacy with less drug. The most widely explored targeted drug delivery strategy for HIV-1 prevention has been topical microbicides. Numerous formulations have been developed as potential rectal and/or vaginal microbicides. Common limitations have included insufficient bioavailability in the tissue, lack of efficacy, or poor tolerability and compliance by the user.[8] Proposed delivery systems have included gels, creams, foams, capsules, enemas, and intravaginal rings. In order to reduce mucosal

inflammation, which can increase HIV-1 infection risk, many studies have examined the inclusion of varying polymers and/or surfactants in carrier gels. While many formulations have shown promising safety and acceptability,[9–11] none has yet advanced to clinical efficacy studies.

Improved delivery of antiretroviral drugs directly to the vulnerable cells mediating transmission of HIV-1 infection may address prior limitations through enhanced bioavailability and therefore better efficacy with less drug. Nanoparticle delivery systems with this goal have included dendrimers with inherent antiviral activity,[12, 13] polymer-based nanoparticles such as poly(lactic-co-glycolic acid),[14–19] and lipid-based nanoparticles or liposomes.[20–22] Benefits include the ability to traverse the mucus layer due to small size that increases distribution and retention,[18] and increased intracellular uptake of drug-loaded particles.[23, 24] For example, dapivirine-loaded poly(ε-caprolactone) nanoparticles, created using a solvent displacement method, are readily internalized by relevant HIV-1 target cells and show at least similar antiviral activity as free drug *in vitro*[14] and surface engineering can ensure efficient penetration and retention in *ex vivo* mucosal studies.[15] Harnessing novel targeted nanodelivery vehicles for HIV-1 prevention is a key area of continued clinical interest.

Currently, oral tenofovir (TFV) disoproxil fumarate/emtricitabine fixed dose combination is the only FDA-approved drug for PrEP use,[25] and long-term risks of TFV (a reverse transcriptase inhibitor) include renal toxicity and decreased bone mineral density.[26–29] Given these potential adverse effects, locally targeted delivery of TFV has been a topic of significant interest; it was the first effective topical HIV-1 prevention drug,[30] and the majority of nanodelivery studies have focused on this drug.[16, 19, 20, 31, 32] Other drugs generally have been selected based on hydrophobicity or other properties relevant for drug encapsulation. These have included protease inhibitors (indivavir[33], saquinavir[19, 23]), non-nucleoside reverse transcriptase inhibitors (efavirenz[18, 19], dapivirine[14, 15]), and other nucleoside reverse transcriptase inhibitors including zidovudine (AZT). AZT was the first FDA-approved drug to treat HIV-1, and while highly effective is now less utilized due to systemic toxicities such as macrocytic anemia, granulocytopenia, myopathy, and mitochondrial toxicity.[34, 35] Its hydrophilic nature made it an attractive drug for initial feasibility studies of nanoparticle encapsulation,[36–39] including one study with using non-covalent coating of nanoparticles.[40] More recently, a few studies have examined the newest class of antiretroviral drugs, integrase strand transfer inhibitors, including elvitegravir (EVG)[16] and bictegravir.[17] EVG is well-tolerated, but undergoes rapid hepatic metabolism, requiring co-administration with an additional drug to inhibit its metabolism. All of these studies have focused on polymer or lipid nanoparticles, and employed methods such as oil in water emulsification or solvent displacement for nanoparticle encapsulation. Only prior studies using dendrimers utilized chemical conjugation for drug loading.[13]

Vault nanoparticles are highly conserved ribonucleoprotein particles that are expressed in most eukaryotic cells,[41, 42] yet their precise biological function remains unclear. Human vaults are barrel-shaped particles with outer shells comprised of 78 copies of the major vault protein (MVP), which align non-covalently C- to N-terminus to provide the overall vault structure.[43, 44] Naturally occurring vaults contain two additional proteins, vault

poly(ADPribose) polymerase (VPARP) and telomerase-associated protein 1 (TEP1), in addition to several copies of small untranslated vault associated RNAs.[45–47] Cellular expression of MVP alone is sufficient to form recombinant vault structures that can be loaded with certain molecules *in vitro*.[48–50]

Recombinant vaults have been engineered for the purposes of vaccination,[51, 52] enzyme delivery,[53, 54] targeting of cell surface receptors,[55] and local delivery of an immunotherapeutic for lung cancer.[49] Although it is known that vaults can be engulfed by certain cells,[56] the precise cell types that naturally take up vaults have not been fully defined. While protein packaging into recombinant vaults has been achieved through fusion with an interaction domain from VPARP that binds to a site on MVP within the interior of vaults,[57] it is more challenging to achieve packaging of small molecule drugs. Although highly hydrophobic molecules have been loaded into recombinant vaults engineered to have internal hydrophobic domains,[48] size, polarity, and solubility generally limit loading of vaults with drugs. Due to these limitations, we sought to examine the feasibility of using vault nanoparticles as a drug-targeting vehicle via drug conjugation rather than encapsulation.

In this study, we find that the natural targets of vault uptake are cells that are highly relevant to the pathogenesis of HIV-1 infection and transmission, and we employ a novel approach to using vaults for drug delivery, by conjugation of antiretroviral drugs to human recombinant vault nanoparticles to achieve targeted drug delivery to inhibit infection of the key cell types involved in HIV-1 transmission.

RESULTS AND DISCUSSION

Vaults are efficiently internalized by antigen-presenting cells and activated T cells within human peripheral blood mononuclear cells.

We examined the ability of different peripheral blood mononuclear cell (PBMC) lineages to engulf vaults by using fluorescence-labeled recombinant human vaults. Human PBMC readily took up recombinant vaults, with maximal uptake achieved by 20 minutes (Figure 1A). To distinguish between cell surface binding versus internalization we compared uptake at 4°C versus 37°C in the presence or absence of trypan blue, an extracellular fluorescence quencher. With trypan blue, cellular fluorescence upon exposure to fluorescent vaults was abolished at 4°C but not 37°C, suggesting that vaults are fully internalized by PBMC (Figure 1B).

The cell types within PBMC mediating vault internalization were further characterized using flow cytometry. The majority (77%) of cells taking up vaults were innate immune antigen presenting cells (APCs), specifically dendritic cells ($CD3^-CD19^-CD11c^+HLA\text{-}DR^+$) and monocytes/macrophages ($CD3^-CD19^-CD14^+HLA\text{-}DR^+CD11c^-$). A subset of B cells ($CD27^-IgD^+$ naïve B cells), which can also function as APCs, also readily internalized vaults. Among T cells, primarily activated ($CD38^+$) T cells were observed to internalize vaults, and nearly all (>90%) activated $CD4^+$ T cells internalized vaults (Figure 2).

As APCs and activated T cells are both capable of endocytosis and phagocytosis, these results suggested that either process could be a mechanism by which exogenous vaults are selectively taken up into these cells, consistent with prior work showing internalization and co-localization of vaults in the lysosome in the endocytic THP-1 human monocytic cell line.[56] Binding saturation experiments using fluorescent vaults were inconclusive due to requirement for high vault concentrations (data not shown), and it was thus unclear whether vault uptake by these specific cells types is receptor mediated or nonspecific endocytosis or phagocytosis.

Selection of antiretroviral drugs for direct conjugation to recombinant vault nanoparticles.

The subsets of PBMC to which vaults naturally target are also the key target cells for HIV-1 infection. As such, we tested the utility of using recombinant vaults for antiretroviral drug delivery. While vaults have been engineered to package highly hydrophobic molecules,[48] available antiretroviral drugs against HIV-1 were not sufficiently hydrophobic to employ this method. Alternatively, we selected drugs that were amenable to direct conjugation to the vault, based on having reactive groups that would be either easily modifiable or directly available for protein conjugation using high-efficiency coupling methods. These included FDA-approved drugs from two clinically relevant antiretroviral drug classes, the nucleoside reverse transcriptase inhibitors and integrase strand transfer inhibitors. Specifically, the drugs chosen were zidovudine (AZT), tenofovir (TFV), and elvitegravir (EVG). For which we employed ester-, carbonate-, and carbamate- based conjugation strategies, respectively. These chemistries were chosen to provide a hydrolytically and/or enzymatically cleavable linkage, allowing slow and sustained release of active drug, offering the potential advantage of better regulating release kinetics compared to typical non-covalent encapsulation strategies. Additionally, this approach provided a direct route to modify the limited functional handles available on the selected drugs.

Modification and conjugation of zidovudine to recombinant human vault nanoparticles.

AZT was suitable for vault conjugation due to the presence of a single hydroxyl group at the 5’ position of the nucleoside, facilitating modifications without unwanted side products. We first added a succinate group through an ester linkage by reacting the 5’ hydroxyl group to succinic anhydride[58] (Scheme 1). This linkage provided relative stability while allowing susceptibility to hydrolysis under acidic conditions or by esterases or nucleases, conditions present in the endosome and cytoplasm of cells,[59, 60] to regenerate the 5’ hydroxyl group in the active form of AZT. This modified drug molecule was then utilized for conjugation to the 3432 free amine groups on vaults (43 lysine amine groups and an unmodified N-terminal amine per MVP, and 78 MVPs per vault).[50] The carboxyl end of the functionalized AZT succinate was converted to an N-hydroxysuccinimide ester (AZT-NHS) using N,N’-dicyclohexylcarbodiimide (DCC) and N-hydroxysuccinimide (NHS)[58] (Scheme 1).

This NHS ester was then conjugated to vaults through amide linkages to free amino groups on lysine (ε-amino) or N-termini (Scheme 2) using 3.28 molar equivalents of AZT-NHS with respect to vault amines, resulting in an average of 1296 ± 3 AZT molecules per vault (37.8% derivatization of the 3432 vault amines) (Table 1). This efficiency exceeded a prior estimate that 9–16% of these vault amines are available for reactivity by NHS coupling.[50]

High performance liquid chromatography (HPLC) studies showed that the ester linkage between the AZT-vault was stable in Dulbecco's phosphate-buffered saline (DPBS) over 24 hours at ambient temperature (data not shown).

Modification and conjugation of tenofovir to recombinant human vault nanoparticles.

Due to limited oral bioavailability, tenofovir is administered as a prodrug either tenofovir disoproxil fumarate (TDF) or tenofovir alafenamide fumarate (TAF).[61] Initial attempts were made to conjugate cleavable linkers to the exocyclic amine of TDF or TAF, but were unsuccessful due to the limited options of cleavable linkers that could be added to this amine. To circumvent this problem, we designed a novel tenofovir prodrug containing an oxycarbonyloxymethyl linker, similar to the linker found on TDF (Scheme 3). In place of the inert terminal isopropyl groups on TDF we used norbornene, providing a stable and orthogonal functional handle for conjugation of the prodrug to vaults. This was accomplished by alkylative esterification of TFV using norbornene methyl(chloromethyl) carbonate to yield tenofovir-di-methylcarbonatemethlynorbornene (TFV-Nor) (Scheme 3) to create a prodrug that can undergo esterase hydrolysis in a manner similar to TDF.

A methyltetrazine-PEG_4-NHS ester linker was used to conjugate TFV-Nor to vaults, requiring a two-part reaction. First, the linker was attached to vault proteins by reacting the NHS ester of the linker with free amines of the vault. This yielded vaults that were heavily decorated with methyltetrazine for selective reactivity with the norbornene of TFV-Nor through an irreversible inverse-electron-demand Diels-Alder reaction[62, 63] (Scheme 4). Vault conjugation was then performed using 5 molar equivalents of TFV-Nor with respect to vault amines, resulting in an average of 640 ± 4 TFV molecules per vault (18.8% derivatization of vault amines) (Table 1).

This conjugation efficiency was lower than AZT for two potential reasons. First, TFV-Nor is significantly more hydrophobic than AZT-NHS, which likely led to increased aggregation of vault proteins when higher conjugation efficiencies were achieved. Second, having two tetrazine-reactive norbornene groups per molecule of TFV may have cross-linked vaults, leading to loss of some vault particles. Despite these potential challenges, our TFV conjugation strategy still resulted in reasonable conjugation efficiency.

Modification and conjugation of elvitegravir to recombinant human vault nanoparticles.

In addition to the two previous reverse transcriptase inhibitor drugs, we selected the integrase strand transfer inhibitor EVG, which contains a readily modifiable primary hydroxyl group amenable to an amine-reactive conjugation strategy analogous to AZT-NHS. However, the presence of a carboxylic acid on EVG precluded modification with an activated ester. Alternatively, EVG was reacted with N,N'-disuccinimidyl carbonate to create the N-hydroxysuccinimidyl carbonate of elvitegravir (EVG-NHS, Scheme 5).

Vault conjugation through carbamate linkages was then performed using 0.3 molar equivalent of EVG-NHS with respect to vault amines (Scheme 6), resulting in 67 ± 5 EVG molecules per vault (1.9% derivatization of vault amines, Table 1). Being a more hydrophobic drug compared to AZT and TFV, EVG demonstrated the lowest conjugation efficiency as expected. Titration experiments showed that as the drug to amine ratio

increased, overall vault recovery decreased, suggesting that increased hydrophobicity imparted by EVG conjugation to the vaults caused them to precipitate. This phenomenon has similarly been reported for antibody-drug conjugates.[64–67]

Antiretroviral drug-conjugated vaults effectively inhibit HIV-1 infection in human PBMC.

To evaluate whether our drug-conjugated vaults access the intracellular compartment and release active drug where they mediate antiviral activity, we compared equivalent amounts of each drug in vault-conjugated versus free forms for the inhibition of *in vitro* HIV-1 infection of human PBMC. All drug-vault conjugates were similarly effective compared to free drug (Figure 3), indicating that vaults taken up intracellularly released the active form of drug for access to the cytoplasm. These results were not due to residual free drug in our vault conjugates, as multiple purification steps were performed and none was detectable by HPLC analyses (data not shown).

While the targeted drug-vault conjugates might have been predicted to have higher potency compared to free drug, lack of this finding may be related to the assay, where direct exposure of PBMC to free drug *in vitro* would minimize any comparative advantage of vault targeting. Drug-targeting via vault conjugation could be advantageous *in vivo* where the key cells for HIV-1 infection are found in lower concentrations within tissues. A possible caveat is that drug conjugation interfered with vault uptake into the relevant target cells for HIV-1 infection, but this seems unlikely for two reasons. First, the experiments showing intracellular uptake of vaults utilized similar chemistry for fluorescent dye conjugation. Second, drug conjugation to the vaults should have been relatively stable extracellularly, yet the active site of the drugs is intracellular. Although the precise mechanism of drug release for these conjugates remains unknown, drug release likely is facilitated enzymatically, by pH-induced hydrolysis, or some combination thereof. It has also been demonstrated in the context of other protein-drug conjugates (such as some antibody-drug conjugates) that release of the drug is not always required for full drug activity,[68] so it is possible that the antiretroviral drugs are active as conjugates or peptide adducts.

Additionally, a prior study showed that enhanced activity was only seen for specific drug combination deliveries, but not for single drugs.[24] We initially focused on single drugs since targeted drug delivery will most likely have immediate clinical utility in HIV-1 prevention (for which single agents may suffice); future studies will include combinations of drugs. Finally, vault nanoparticles can be engineered to have antibody-specific targeting,[55] and engineering CD4-targeted vaults could further improve targeting to HIV-1-susceptible cells. Others have used CD4 targeting strategies to improve nanodelivery of indinavir for HIV-1 infection.[33]

Overall, our data have shown that functional drug can be effectively delivered via conjugation to recombinant human vault nanoparticles, which are naturally self-targeted to the key cells involved in HIV-1 infection, potentially improving efficacy and minimizing systemic toxicity.

CONCLUSIONS

This study identified specific subsets of immune cells that readily take up human vault nanoparticles, predominantly antigen presenting cells (dendritic cells, monocytes/macrophages) and activated T cells. Because these are the key cell types infected by HIV-1, this suggests that vault targeting could be harnessed for antiretroviral drug delivery for HIV-1 prevention or treatment strategies to maximize efficacy while minimizing systemic toxicity. As proof of concept, three anti-HIV-1 drugs were each directly conjugated to recombinant human vault nanoparticles. These vault-conjugated drugs retained antiviral activity against HIV-1 infection of PBMC, indicating intracellular access and release of active drug. This delivery system could facilitate targeted drug delivery for HIV-1 prevention (e.g. microbicides) or enhanced treatment strategies.

EXPERIMENTAL PROCEDURES (MATERIALS AND METHODS)

Recombinant human vault preparation.

Recombinant human vault particles were purified from baculovirus infected Sf9 insect cell pellets. Briefly, baculovirus infected Sf9 cells were lysed on ice in buffer A [50 mM Tris-HCl (pH 7.4), 75 mM NaCl, and 0.5 mM $MgCl_2$] with 1% Triton X-100, 1 mM DTT, 0.5 mM PMSF, and protease inhibitor cocktail (Sigma 8849). Lysates were dounced on ice and centrifuged at 20,000g for 20 minutes. The supernatant fraction was then centrifuged at 100,000g for 1 hour to pellet the vaults. Following resuspension, the vault particles were purified by sucrose gradient as described previously.[69]

Fluorescent vault labeling and uptake.

Purified recombinant human vaults were fluorescently labeled using DyLight-488 amine-reactive dye according to manufacturer's recommendations (Thermo Scientific). For uptake studies, human peripheral blood mononuclear cells (PBMC) were obtained from de-identified donors through the UCLA Center for AIDS Research Virology Core. Fluorescent vaults at a concentration of 1 μg/ml were incubated with 1×10^6 PBMC in RPMI/10% FBS for indicated times (5 min to 2 hours) at 37°C then immediately fixed in 2% paraformaldehyde or placed on ice for flow cytometry staining. For the trypan blue experiments, 0.4 mg/ml trypan blue was added to the sample immediately prior to data acquisition on the flow cytometer.

Flow cytometry.

PBMC were stained in PBS with 1% human AB serum for 30 minutes on ice using fluorescent-conjugated antibodies as described in detail in Supporting Information. Cells were washed with cold PBS at 10X the staining volume then fixed using 1% paraformaldehyde. Data was acquired on a Becton Dickinson LSRFortessa cytometer and analyzed using FlowJo v10 (FlowJo, LLC). Live cells were gated using Live/Dead Aqua (Life Technologies) and singlets gated with FSC-H and FSC-A parameters. Following this a large lymphocyte cell gate was created by forward and side scatter parameters. Vault+ gates were determined using "no vault" conditions as background, and all other staining gates based on isotype controls.

Chemical materials.

Triethylamine (TEA) and N-methyl-2-pyrrolidone (NMP) were dried with 3 Å molecular sieves and then distilled prior to use. Tetrahydrofuran (THF), acetonitrile (MeCN), and dichloromethane (DCM) were dried by purging with nitrogen and passage through activated alumina columns prior to use. Zidovudine and tenofovir were purchased from Combi-Blocks, elvitegravir from eNovation Chemicals, and the methyltetrazine-PEG_4-NHS ester linker from Click Chemistry Tools. All other chemicals were used as purchased unless otherwise noted from Acros, Alfa Aesar, Sigma Aldrich, Chem-Impex, or Fisher Scientific.

Analytical techniques.

NMR spectra were obtained using either Bruker AV400 or Bruker AV500 spectrometer. ESI mass spectra were obtained using either a Waters Acquity LCT Premier XE equipped with an autosampler and direct injection port or an Agilent 6530 QTOF-ESI with a 1260 Infinity LC with autosampler. Analytical reverse phase high performance liquid chromatography (HPLC) was carried out on a Agilent 1260 Infinity II HPLC system equipped with an autosampler and a UV detector using a Poroshell 120 2.7 μm C18 120 Å column (analytical: 2.7 μm, 4.6 × 100 mm) with monitoring at λ = 220 and 280 nm and with a flow rate of 0.8 ml/min. Preparatory reverse phase HPLC was carried out on a Shimadzu high performance liquid chromatography system equipped with a UV detector using a Luna 5 μm C18 100 Å column (preparatory: 5 μm, 250 × 21.2 mm) with monitoring at λ = 215 and 254 nm and with a flow rate of 20 ml/min.

Synthesis of AZT succinate.

The synthesis of AZT succinate was accomplished by modifying a preexisting procedure.[58] Succinic anhydride (0.120 g, 1.19 mmol, 1.6 eq) was added to a round bottom flask containing a stirring solution of AZT (0.200 g, 0.75 mmol, 1.0 eq) in THF (10 mL). After succinic anhydride was fully dissolved, TEA (0.184 mL, 1.32 mmol, 1.8 eq) was slowly added to the flask. The reaction mixture was refluxed for 16 hours and was then concentrated under reduced pressure. Excess succinic anhydride was removed by dissolving the dried reaction content in DI water (20 mL) and ethyl acetate (EtOAc) (20 mL). The aqueous layer was basified to pH 7.0 using 3.0 M NaOH and succinic anhydride was extracted with 3 X EtOAc (20 mL). The aqueous layer was then adjusted to pH 3.0 using concentrated HCl and the product was extracted using 3 X EtOAc (20 mL). The organic fractions were collected, dried with anhydrous sodium sulfate, and concentrated under reduced pressure. Final purification was accomplished using silica flash column chromatography, 20% methanol (MeOH)/EtOAc to yield a white solid (0.203 g, 73.7% yield). See Supporting Information Figure S1 for ^{1}H NMR (400 MHz, $CDCl_3$, 25 °C): δ 10.64–10.53 (br s, 1H), 7.44 (d, *J* = 1.1 Hz, 1H), 5.91 (td, *J* = 5.7, 1.4 Hz, 1H), 4.79 (dd, *J* = 12.7, 1.7 Hz, 1H), 4.34 (dt, *J* = 7.2, 4.0 Hz, 1H), 4.28 (dd, J = 12.7, 3.8 Hz, 1H), 4.11 (td, *J* = 3.9, 1.7 Hz, 1H), 2.92–2.81 (m, 1H), 2.77–2.57(m, 4H), 2.40 (ddd, *J* = 13.8, 6.7, 5.1 Hz, 1H), 1.87 (d, *J* = 1.1, 3H). See Supporting Information Figure S2 for ^{13}C NMR (100 MHz, $CDCl_3$, 25 °C): δ 177.9, 172.8, 166.5, 149.5, 137.6, 109.8, 85.9, 83.0, 63.2, 60.3, 38.1, 29.0, 28.8, 12.5. FTIR: ν = 3177, 3021, 2934, 2103, 1682, 1651, 1473, 1407, 1365, 1321, 1267,

1156, 1096, 1064, 997, 957, 895, 829, 776 cm^{-1}. HRMS: Calc. [M-1] = 366.1050 Da; Obs. [M-1] = 366.1108 Da.

Synthesis of AZT-NHS.

AZT succinate (0.506 g, 1.37 mmol, 1.0 eq), NHS (0.153 g, 1.37 mmol, 1.0 eq), and dicyclohexylcarbodiimide (DCC) (0.270 g, 1.37 mmol, 1.0 eq) were placed in a Schlenk flask and dissolved in THF (30 mL). The reaction was performed under nitrogen, cooled to 0 °C, and stirred for 2 hours. This led to a heterogeneous reaction mixture, which was concentrated under reduced pressure to yield a white solid. The product was purified using silica flash column chromatography, 0% EtOAc/hexanes to 100% EtOAc/hexanes. The sample was then crystallized 4 X, 40% DCM/hexanes to remove excess DCC. Preparative HPLC was performed to remove excess NHS to yield a white solid (0.416 g, 65.0% yield). See Supporting Information Figure S3 for ^{1}H NMR (400 MHz, $CDCl_3$, 25 °C): δ 9.22–9.09 (br s, 1H), 7.24 (d, *J* = 1.1 Hz, 1H), 6.07 (t, *J* = 6.4 Hz, 1H), 4.44 (dd, *J* = 12.2, 4.3 Hz, 1H), 4.36 (dd, *J* = 12.2, 3.8 Hz, 1H), 4.24 (dt, *J* = 7.4, 5.7 Hz, 1H), 4.04 (dt, *J* = 5.5, 4.1 Hz, 1H), 3.04–2.95 (m, 2H), 2.84 (s, 4H), 2.81 (t, *J* = 6.6 Hz), 2.53–2.35 (m, 2H), 1.93 (d, J = 1.1 Hz, 3H). See Supporting Information Figure S4 for ^{13}C NMR (100 MHz, $CDCl_3$, 25 °C): δ 170.7, 169.1, 167.9, 164.2, 150.1, 136.2, 111.4, 85.9, 81.8, 63.6, 60.3, 37.5, 28.9, 26.4, 25.7, 12.6. FTIR: ν = 3190, 3021, 2970, 2106, 1813, 1782, 1733, 1682, 1471, 1407, 1365, 1316, 1261, 1202, 1089, 1068, 1046, 995, 959, 892, 849, 805 cm^{-1}. HRMS: Calc. [M+1] = 465.1370 Da; Obs. [M+1] = 465.1429 Da. High-resolution mass spectrometry (HRMS) of final AZT-NHS product is shown in Supporting Information Figure S11.

Synthesis of norbornene methyl (chloromethyl) carbonate.

TEA (0.868 mL, 6.20 mmol, 1.5 eq) was slowly added to a 0 °C solution of 5-norbornene-2-methanol (0.50 mL, 4.14 mmol, 1.0 eq) in DCM (20 mL). After 5 minutes, chloromethyl chloroformate (0.40 mL, 4.55 mmol, 1.1 eq) was added dropwise and the reaction mixture was allowed to come to room temperature and stir for 2 hours. The reaction was quenched with DI water (20 mL) and the product was extracted using 4 X DCM (20 mL). The organic fractions were combined, dried using anhydrous sodium sulfate, and concentrated under reduced pressure. The product was purified using silica flash column chromatography, 0% EtOAc/hexanes to 5% EtOAc/hexanes. Fractions were concentrated under reduced pressure to yield a light yellow oil which was vacuum distilled to give a colorless oil (0.585 g, 65.3% yield). See Supporting Information Figure S5 for ^{1}H NMR (400 MHz, $CDCl_3$, 25 °C): δ 6.18 (dd, *J* = 5.7, 3.0 Hz, 0.7H), 6.09 (t, *J* = 1.6 Hz, 0.6H), 5.96 (dd, *J* = 5.7, 2.9 Hz, 0.7H), 5.74 (s, 0.6H), 5.73 (d, *J* = 0.6 Hz, 1.3H), 4.30 (dd, *J* = 10.6, 6.4 Hz, 0.3H), 4.13 (dd, *J* = 10.6, 9.3 Hz, 0.3H), 4.00 (dd, *J* = 10.4, 6.7 Hz), 3.82 (dd, *J* = 10.4, 9.5 Hz, 0.7H), 2.95 – 2.88 (br s, 0.7 H), 2.88 – 2.80 (br s, 1H), 2.77 – 2.72 (br s, 0.3H), 2.51 – 2.41 (m, 0.7H), 1.88 (dd, *J* = 9.2, 3.8 Hz, 0.4H), 1.85 (dd, *J* = 9.2, 3.8 Hz, 0.4H), 1.83 – 1.75 (m, 0.3H), 1.55 (s, 0.2H), 1.85 (dd, *J* = 9.2, 3.8 Hz, 0.3H), 1.48 (dd, *J* = 4.1, 2.0 Hz, 0.4H), 1.39 (td, *J* = 3.3, 1.7 Hz, 0.1H), 1.37 (td, *J* = 1.62, 0.6 Hz, 0.2H), 1.34 −1.33 (m, 0.1H), 1.32 – 1.31 (br s, 0.2H), 1.31 – 1.29 (m, 0.2H), 1.29 – 1.27 (br s, 0.5H), 1.27 – 1.25 (br s, 0.3H), 1.19 (dd, *J* = 4.4, 3.5 Hz, 0.2H), 1.16 (dd, *J* = 4.4, 3.5 Hz, 0.1H) 0.57 (ddd, *J* = 11.8, 4.4, 2.6 Hz, 0.7H). See Supporting Information Figure S6 for ^{13}C NMR (100 MHz, $CDCl_3$, 25 °C): δ 153.6, 153.5, 138.1, 137.2, 136.2, 132.2, 73.3, 72.7, 72.3, 72.3, 49.6, 45.1, 43.9, 43.6, 42.3, 41.7,

38.1, 37.8, 29.5, 28.9. FTIR: ν = 3061, 2968, 2870, 1761, 1570, 1444, 1390, 1341, 1326, 1239, 1226, 1153, 1110, 1025, 1012, 992, 978, 958, 928, 882, 858, 836, 825, 786, 713 cm^{-1}.

Synthesis of TFV-Nor.

Tenofovir (0.210 g, 0.73 mmol, 1.0 eq) and tetrabutylammonium bromide (TBAB) (0.235 g, 0.73 mmol, 1 eq) were added to a Schlenk flask and placed under reduced pressure at 50 °C for 16 hours to remove residual water. NMP (25 mL), TEA (0.41 ml, 2.92 mmol, 4 eq), and norbornene methyl (chloromethyl) carbonate (0.788 g, 3.63 mmol, 5 eq) were added to the reaction flask. The reaction was placed under nitrogen and heated to 50 °C for 2 days. The reaction was cooled to room temperature and concentrated under reduced pressure. The resulting residue was dissolved in DI water (20 mL) and the product was extracted using 4 X EtOAc (20 mL). The organic layers were combined, dried using anhydrous sodium sulfate, and concentrated under reduced pressure. The product was then subjected to silica flash column chromatography, 0% MeOH/EtOAc to 5% MeOH/EtOAc. Fractions were concentrated under reduced pressure to yield a light yellow oil which was further purified using preparative HPLC to give a white solid (0.264 g, 55.7% yield). See Supporting Information Figure S7 for ^{1}H NMR (400 MHz, $CDCl_3$, 25 °C): δ 8.29 (s, 1H), 8.28 (s, 1H), 8.21 – 8.10 (br s, 1H), 6.14 (dd, *J* = 5.6, 3.0 Hz, 1.4H), 6.08 – 6.01 (br s, 1.1H), 5.89 (dd, *J* = 5.4, 2.5 Hz, 1.4H), 5.69 – 5.52 (m, 4H), 4.43 (dd, *J* = 14.4, 2.5 Hz, 1H), 4.28 – 4.11 (m, 1.6H), 4.09 – 3.88 (m, 4.1H), 3.81 – 3.65 (m, 2.4H), 2.89 – 2.83 (br s, 1.5H), 2.83 – 2.74 (br s, 1.9H), 2.69 –2.64 (br s, 0.5H), 2.45 – 2.32 (m, 1.5H), 1.80 (ddd, *J* = 12.0, 9.0, 3.4, Hz, 1.4H), 1.76 – 1.67 (m, 0.6H), 1.47 – 1.39 (m, 1.9H), 1.36 – 1.30 (m, 0.6H), 1.28 – 1.19 (m, 5.6H), 1.12 (dt, *J* = 11.8, 3.9, Hz, 0.6H), 0.52 (m, 1.4H)m. See Supporting Information Figure S8 for ^{13}C NMR (100 MHz, $CDCl_3$, 25 °C): δ 153.78, 153.75, 153.69, 153.66, 151.5, 149.1, 144.8, 144.6, 138.06, 137.2, 136.0, 131.9, 117.9, 117.3, 84.5, 76.3, 76.2, 73.2, 72.6, 63.7, 62.1, 49.5, 48.8, 45.0, 43.8, 43.5, 42.2, 41.6, 38.0, 37.8, 29.4, 28.8, 16.3. FTIR: ν = 3061, 2970, 2872, 1760, 1693, 1515, 1468, 1420, 1387, 1350, 1327, 1248, 1197, 1139, 1038, 1003, 947, 927, 897, 858, 826, 786, 765, 720 cm^{-1}. HRMS: Calc. [M+1] = 648.2435 Da; Obs. [M+1] = 648.2083 Da. HRMS of final TFV-Nor product is shown in Supporting Information Figure S12.

Synthesis of EVG-NHS.

To a previously oven dried 2-neck 25 ml round bottom flask under Argon was added *N,N'*-disuccinimidyl carbonate (0.143 g, 0.53 mmol, 5 eq) and 4 ml dry MeCN. In a separate vial was dissolved EVG (0.050 g, 0.11 mmol, 1 eq) in 3 ml dry MeCN and TEA (0.047 ml, 0.33 mmol, 3 eq) while under Argon. This solution of EVG was briefly mixed and then added dropwise via syringe into the solution of *N,N'*-disuccinimidyl carbonate. The reaction was stirred at 22 °C for 5 hours, then the solvent was completely removed under vacuum. The crude material was purified using preparative HPLC followed by removal of solvent under vacuum to yield a yellow solid (30.93 mg, 46.9% yield). See Supporting Information Figure S9 for ^{1}H NMR (500 MHz, $CDCl_3$, 25 °C): δ 8.73 (s, 1H), 8.25 (s, 1H), 7.25 (dd, *J* = 14.8, 1.4 Hz, 1H), 7.06 (t, *J* =7.1 Hz, 1H), 6.98 (t, *J* = 7.8 Hz, 1H), 6.94 (s, 1H), 4.89 (d, *J* = 9.8 Hz, 1H), 4.73 (m, 2H), 4.10 (q, *J* = 12.9 Hz, 2H), 3.99 (s, 3H), 2.73 (s, 4H), 2.42 (m, 1H), 1.25 (d, *J* = 6.3 Hz, 3H), 0.83 (d, *J* = 6.5 Hz, 3H). See Supporting Information Figure S10 for ^{13}C NMR (126 MHz, $CDCl_3$, 25 °C): δ 177.2, 168.2, 167.9, 163.0, 157.5, 151.3, 143.5,

142.4, 129.42, 129.41, 129.38, 128.96, 128.90, 128.47, 127.83, 127.71, 124.44, 124.40, 121.17, 121.03, 119.7, 109.3, 95.6, 70.0, 64.4, 56.2, 30.8, 29.05, 29.03, 25.4, 19.8, 19.5. FTIR: ν = 2957, 2920, 1814, 1789, 1739, 1613, 1456, 1374, 1305, 1257, 1195, 1152, 1095, 1047, 1012, 991, 923, 878, 810, 790, 753, 732 cm^{-1}. HRMS: Calc. [M+1] = 589.1389 Da; Obs. [M+1] = 589.1391 Da. HRMS of final EVG-NHS product is shown in Supporting Information Figure S13.

Conjugation of AZT-NHS to vaults.

0.5 mg of lyophilized human MVP (hMVP) vaults were resuspended in 125 μl 1x DPBS. 1 μl of 200 μg/μl AZT-NHS stock solution in DMSO was added to 74 μl of 4 μg/μl hMVP vaults in 1 x DPBS. The reaction was incubated at room temperature for 2 hours. AZT conjugated vaults were purified from unconjugated AZT-NHS by gel exclusion chromatography using Bio-Gel® P polyacrylamide P-6 Columns. To further eliminate any potential contamination of the AZT conjugated vaults with free AZT-NHS, a stepwise sucrose gradient (sucrose fractions of 20%, 30%, 40%, 45%, 50% and 60%) was performed. The sucrose gradient was spun at 25K, 16 hours, 4 °C, ω^2t=3.95E11 in a sw41 rotor. Sucrose fractions (40% and 45%) containing AZT conjugated vaults were collected, diluted in 1 x DPBS and spun at 40K for 2 hours, 4 °C in a Ti 70.1 rotor. The resulting AZT-vault pellet was washed with 6.5 ml of 1x DPBS and centrifuged at 40K for 1 h, 4 °C in a Ti70.1 rotor. The wash step was repeated 2x to ensure the complete removal of any residual sucrose. Subsequently, the washed pellet was resuspended in 150 μl of 1x DPBS, filtered via 0.2 μm syringe filter and the protein concentration determined by BCA assay. The concentration of the vaults was found to be 0.81 μg/μl.

Conjugation of TFV-Nor to vaults.

1 mg of lyophilized recombinant human vaults was added 1375 μl DPBS and the lyophilized cake was dissolved by gentle shaking. NHS-TEG-tetrazine linker was then added (125 μl of a 4 μg/μl stock solution prepared in DMSO; 0.50 mg; 0.562 μmol; 2.25 eq./lysine). The reaction was then mixed on a rocker table at 22 °C for 2 hours. The unreacted linker was then removed by centrifugal filtration using a pre-equilibrated 30 kDa MW cutoff filters. The contents were centriprepped 5 times and the products collected by inverse centrifugation. This material was diluted in 1407 μl of DPBS in a new 1.5 ml tube and TFV-Nor was added (93 μl of a 15 μg/μl stock solution prepared in DMSO; 1.40 mg; 2.16 μmol; 5 eq./lysine). Some drug precipitated, but the conjugation was continued on the rocker for 24 hours followed by purification by sucrose gradient as described above. The vaults eluted in the 40 and 45% fractions and were collected and their concentration measured via standard BCA Assay. The concentration of the vaults was found to be 0.554 μg/μl.

Conjugation of EVG-NHS to vaults.

1 mg of lyophilized recombinant human vaults was added 950 μl DPBS, then transferred to a 2 ml LoBind tube. Another 950 μl DPBS was used to wash the tube and also transferred to the 2 ml tube for a total volume of 1900 μl. 23.5 μl DMSO was then added to the 2 ml tube. Then, EVG-NHS was added (76.5 μl of 1 μg/μl stock solution prepared in DMSO; 0.076 mg; 0.13 μmol; 0.3 eq./lysine). The conjugation was gently mixed on a rocker table for 4 hours at 22 °C followed by purification by sucrose gradient as described above. The conjugate eluted

in the 40 and 45% fractions and was collected and its concentration determined to be 1.469 μg/μl via standard BCA Assay.

General procedure for quantification of drug-vault conjugates via HPLC.

An HPLC standard curve for each antiretroviral was generated by measuring the peak area (280 nm absorbance) after injecting, in triplicate, 1, 5, 10, 50, 100, 500, and 1000 ng of each drug and plotting the corresponding peak areas against the amount of drug injected. After generating these standard curves, the average number of drugs per vault was determined for each conjugate via basic hydrolysis of the labile linkages (either ester or carbamate) between drug molecules to release the native drug. The area under the peak corresponding to the retention time of each drug was then used to determine the amount of drug injected, which was then used to calculate the number of drugs attached to each vault. Additionally, a negative control consisting of the conjugate with no NaOH added was used to determine the amount of free drug before basic hydrolysis, and this amount was subtracted from the amount of calculated conjugated drug.

Preparative HPLC.

AZT-NHS was purified using a mobile phase consisting of 10–95% MeCN + 0.1% trifluoroacetic acid (TFA) in water beginning with 1 min isocratic at 10%, then up to 95% over 15 min in a linear gradient, followed by an isocratic hold at 95% MeCN + 0.1% TFA for 4 min (total time was 20 min; product eluted at 13.5 min). TFV-Nor was purified using a mobile phase consisting of 40–95% MeCN + 0.1% TFA in water beginning with 1 min isocratic at 40%, then up to 95% over 15 min in a linear gradient, followed by an isocratic hold at 95% MeCN + 0.1% TFA for 4 min (total time was 20 min; product eluted at 12.0 min). EVG-NHS was purified using a mobile phase consisting of 50–95% MeCN + 0.1% TFA in water beginning with 1 min isocratic at 50%, then up to 95% over 15 min in a linear gradient, followed by an isocratic hold at 95% MeCN + 0.1% TFA for 4 min (total time was 20 min; product eluted at 15.8 min).

Analytical HPLC.

Zidovudine was analyzed using a mobile phase consisting of 10–100% MeCN + 0.1% TFA in water beginning with a 1 min isocratic at 10%, then up to 100% over 10 min in a linear gradient, followed by an isocratic hold at 100% MeCN + 0.1% TFA for 4 min (total time was 15 min; product eluted at 5.9 min). Tenofovir was analyzed using a mobile phase consisting of 5–100% MeCN + 0.1% TFA in water beginning with 5 min isocratic at 5%, then up to 100% over 6 min in a linear gradient, followed by an isocratic hold at 100% MeCN + 0.1% TFA for 4 min (total time was 15 min; product eluted at 3.1 min). Elvitegravir was analyzed using a mobile phase consisting of 10–100% MeCN + 0.1% TFA in water beginning with a 1 min isocratic at 10%, then up to 100% over 10 min in a linear gradient, followed by an isocratic hold at 100% MeCN + 0.1% TFA for 4 min (total time was 15 min; product eluted at 11.0 min).

HIV-1 stock preparation.

The following reagent was obtained from the NIH AIDS Reagent Program, Division of AIDS, National Institute of Allergy and Infectious Diseases (NIAID), NIH: HIV-1_{BaL} from Dr. Suzanne Gartner, Dr. Mikulas Popovic and Dr. Robert Gallo. Stocks of HIV-1_{BaL} were prepared by infection using PBMC from multiple HIV-1-uninfected donors. Virus titer was determined by titration using Rev response element (RRE)-GFP reporter T1 cells. The same viral stock was used throughout the study.

HIV-1 infection of PBMC and intracellular p24 staining.

Activated PBMC were pre-incubated with indicated concentration of antiretroviral drug or drug-vault conjugate for two hours at 37°C. PBMC (1×10^5 cells) were infected in duplicate with 0.5 multiplicity of infection (MOI) HIV-1_{BaL} for two hours at 37°C then washed three times with RPMI and plated in 48-well plates. Cultures were maintained in RPMI/10% FBS for 5 days then cells were harvested for intracellular p24. Staining was performed using Fix/PERM kit (R&D Systems) and KC57 (clone FH190-1-1)-PE conjugated antibody (Coulter) according to manufacturer's instructions then fixed in 2% paraformaldehyde until flow cytometry acquisition. Data was acquired using a FACScan flow cytometer (Becton Dickinson) and analyzed using FlowJo v10 (FlowJo, LLC). Infection was quantified as percent of cells with p24 expression then normalized to 100% infection using the control infection (no drug) for each independent experiment.

Supplementary Material

Refer to Web version on PubMed Central for supplementary material.

ACKNOWLEDGMENTS

The authors thank C. Hendrix and L. Rohan for helpful discussions. This study was supported by the National Institute of Allergy and Infectious Diseases of the National Institutes of Health R01AI112016 (O.O.Y) and a grant from the AIDS Healthcare Foundation. The content is solely the responsibility of the authors and does not necessarily represent the official views of the National Institutes of Health. Additional support was provided by the UCLA AIDS Institute and Center for AIDS Research (P30 AI028697), James B. Pendleton Trust, and the McCarthy Foundation. The authors declare the following competing financial interest(s): V.A.K., L.H.R., and O.O.Y. have financial interest in Vault Nano Inc., which has licensed intellectual property used in this study from the Regents of the University of California.

ABBREVIATIONS

HIV-1	Human Immunodeficiency Virus-1
MVP	major vault protein
VPARP	vault poly(ADPribose) polymerase
TEP1	telomerase-associated protein 1
PBMC	peripheral blood mononuclear cells
AZT	zidovudine
TFV	tenofovir

EVG	elvitegravir
TEA	triethylamine
DCC	N,N’-dicyclohexylcarbodiimide
NHS	N-hydroxysuccinimide
HPLC	high performance liquid chromatography
DPBS	Dulbecco’s phosphate-buffered saline
TDF	tenofovir disoproxil fumarate
TAF	tenofovir alafenamide fumarate
TFV-Nor	tenofovir-di-methylcarbonatemethlynorbornene
DTT	Dithiothreitol
PMSF	phenylmethylsulfonyl fluoride
NMP	N-methyl-2-pyrrolidone
THF	Tetrahydrofuran
MeCN	acetonitrile
DCM	dichloromethane
EtOAc	ethyl acetate
MeOH	methanol
HRMS	high-resolution mass spectrometry
TBAB	tetrabutylammonium bromide
hMVP	human major vault protein
TFA	trifluoroacetic acid

REFERENCES

(1). Gotwals P, Cameron S, Cipolletta D, Cremasco V, Crystal A, Hewes B, Mueller B, Quaratino S, Sabatos-Peyton C, Petruzzelli L, Engelman JA, and Dranoff G (2017) Prospects for combining targeted and conventional cancer therapy with immunotherapy. Nat Rev Cancer 17, 286–301. [PubMed: 28338065]

(2). World Health Organization. (2018) Global Health Observatory data repository. http://apps.who.int/gho/data/view.main.HIVINCIDENCEREGIONv?lang=en. Accessed on June 24, 2019.

(3). Baeten JM, Donnell D, Ndase P, Mugo NR, Campbell JD, Wangisi J, Tappero JW, Bukusi EA, Cohen CR, Katabira E, Ronald A, Tumwesigye E, Were E, Fife KH, Kiarie J, Farquhar C, John-Stewart G, Kakia A, Odoyo J, Mucunguzi A, Nakku-Joloba E, Twesigye R, Ngure K, Apaka C, Tamooh H, Gabona F, Mujugira A, Panteleeff D, Thomas KK, Kidoguchi L, Krows M, Revall J, Morrison S, Haugen H, Emmanuel-Ogier M, Ondrejcek L, Coombs RW, Frenkel L, Hendrix C,

Bumpus NN, Bangsberg D, Haberer JE, Stevens WS, Lingappa JR, and Celum C (2012) Antiretroviral prophylaxis for HIV prevention in heterosexual men and women. N Engl J Med 367, 399–410. [PubMed: 22784037]

(4). Grant RM, Lama JR, Anderson PL, McMahan V, Liu AY, Vargas L, Goicochea P, Casapia M, Guanira-Carranza JV, Ramirez-Cardich ME, Montoya-Herrera O, Fernandez T, Veloso VG, Buchbinder SP, Chariyalertsak S, Schechter M, Bekker LG, Mayer KH, Kallas EG, Amico KR, Mulligan K, Bushman LR, Hance RJ, Ganoza C, Defechereux P, Postle B, Wang F, McConnell JJ, Zheng JH, Lee J, Rooney JF, Jaffe HS, Martinez AI, Burns DN, and Glidden DV (2010) Preexposure chemoprophylaxis for HIV prevention in men who have sex with men. N Engl J Med 363, 2587–99. [PubMed: 21091279]

(5). Thigpen MC, Kebaabetswe PM, Paxton LA, Smith DK, Rose CE, Segolodi TM, Henderson FL, Pathak SR, Soud FA, Chillag KL, Mutanhaurwa R, Chirwa LI, Kasonde M, Abebe D, Buliva E, Gvetadze RJ, Johnson S, Sukalac T, Thomas VT, Hart C, Johnson JA, Malotte CK, Hendrix CW, and Brooks JT (2012) Antiretroviral Preexposure Prophylaxis for Heterosexual HIV Transmission in Botswana. New England Journal of Medicine 367, 423–434. [PubMed: 22784038]

(6). Zhang Z, Schuler T, Zupancic M, Wietgrefe S, Staskus KA, Reimann KA, Reinhart TA, Rogan M, Cavert W, Miller CJ, Veazey RS, Notermans D, Little S, Danner SA, Richman DD, Havlir D, Wong J, Jordan HL, Schacker TW, Racz P, Tenner-Racz K, Letvin NL, Wolinsky S, and Haase AT (1999) Sexual transmission and propagation of SIV and HIV in resting and activated CD4+ T cells. Science 286, 1353–7. [PubMed: 10558989]

(7). Patterson KB, Prince HA, Kraft E, Jenkins AJ, Shaheen NJ, Rooney JF, Cohen MS, and Kashuba AD (2011) Penetration of tenofovir and emtricitabine in mucosal tissues: implications for prevention of HIV-1 transmission. Sci Transl Med 3, 112re4.

(8). Traore YL, Chen Y, and Ho EA (2018) Current State of Microbicide Development. Clin Pharmacol Ther 104, 1074–1081. [PubMed: 30107032]

(9). Anton PA, Saunders T, Elliott J, Khanukhova E, Dennis R, Adler A, Cortina G, Tanner K, Boscardin J, Cumberland WG, Zhou Y, Ventuneac A, Carballo-Diéguez A, Rabe L, McCormick T, Gabelnick H, Mauck C, and McGowan I (2011) First Phase 1 Double-Blind, Placebo-Controlled, Randomized Rectal Microbicide Trial Using UC781 Gel with a Novel Index of Ex Vivo Efficacy. PLoS One 6, e23243.

(10). Anton PA, Cranston RD, Kashuba A, Hendrix CW, Bumpus NN, Richardson-Harman N, Elliott J, Janocko L, Khanukhova E, Dennis R, Cumberland WG, Ju C, Carballo-Dieguez A, Mauck C, and McGowan I (2012) RMP-02/MTN-006: A phase 1 rectal safety, acceptability, pharmacokinetic, and pharmacodynamic study of tenofovir 1% gel compared with oral tenofovir disoproxil fumarate. AIDS Res Hum Retroviruses 28, 1412–21. [PubMed: 22943559]

(11). McGowan I, Cranston RD, Duffill K, Siegel A, Engstrom JC, Nikiforov A, Jacobson C, Rehman KK, Elliott J, Khanukhova E, Abebe K, Mauck C, Spiegel HM, Dezzutti CS, Rohan LC, Marzinke MA, Hiruy H, Hendrix CW, Richardson-Harman N, and Anton PA (2015) A Phase 1 Randomized, Open Label, Rectal Safety, Acceptability, Pharmacokinetic, and Pharmacodynamic Study of Three Formulations of Tenofovir 1% Gel (the CHARM-01 Study). PLoS One 10, e0125363.

(12). Telwatte S, Moore K, Johnson A, Tyssen D, Sterjovski J, Aldunate M, Gorry PR, Ramsland PA, Lewis GR, Paull JR, Sonza S, and Tachedjian G (2011) Virucidal activity of the dendrimer microbicide SPL7013 against HIV-1. Antiviral Res 90, 195–9. [PubMed: 21459115]

(13). Arnáiz E, Vacas-Córdoba E, Galán M, Pion M, Gómez R, Muñoz-Fernández MÁ, and de la Mata FJ (2014) Synthesis of anionic carbosilane dendrimers via “click chemistry” and their antiviral properties against HIV. Journal of Polymer Science Part A: Polymer Chemistry 52, 1099–1112.

(14). das Neves J, Michiels J, Arien KK, Vanham G, Amiji M, Bahia MF, and Sarmento B (2012) Polymeric nanoparticles affect the intracellular delivery, antiretroviral activity and cytotoxicity of the microbicide drug candidate dapivirine. Pharm Res 29, 1468–84. [PubMed: 22072053]

(15). das Neves J, Araujo F, Andrade F, Michiels J, Arien KK, Vanham G, Amiji M, Bahia MF, and Sarmento B (2013) In vitro and ex vivo evaluation of polymeric nanoparticles for vaginal and rectal delivery of the anti-HIV drug dapivirine. Mol Pharm 10, 2793–807. [PubMed: 23738946]

(16). Mandal S, Prathipati PK, Kang G, Zhou Y, Yuan Z, Fan W, Li Q, and Destache CJ (2017) Tenofovir alafenamide and elvitegravir loaded nanoparticles for long-acting prevention of HIV-1 vaginal transmission. AIDS 31, 469–476. [PubMed: 28121666]

(17). Mandal S, Prathipati PK, Belshan M, and Destache CJ (2019) A potential long-acting bictegravir loaded nano-drug delivery system for HIV-1 infection: A proof-of-concept study. Antiviral Res 167, 83–88. [PubMed: 30991088]

(18). Nunes R, Araujo F, Barreiros L, Bartolo I, Segundo MA, Taveira N, Sarmento B, and das Neves J (2018) Noncovalent PEG Coating of Nanoparticle Drug Carriers Improves the Local Pharmacokinetics of Rectal Anti-HIV Microbicides. ACS Appl Mater Interfaces 10, 34942–34953. [PubMed: 30234288]

(19). Chaowanachan T, Krogstad E, Ball C, and Woodrow KA (2013) Drug synergy of tenofovir and nanoparticle-based antiretrovirals for HIV prophylaxis. PLoS One 8, e61416.

(20). Perazzolo S, Shireman LM, Koehn J, McConnachie LA, Kraft JC, Shen DD, and Ho RJY (2018) Three HIV Drugs, Atazanavir, Ritonavir, and Tenofovir, Coformulated in Drug-Combination Nanoparticles Exhibit Long-Acting and Lymphocyte-Targeting Properties in Nonhuman Primates. J Pharm Sci 107, 3153–3162. [PubMed: 30121315]

(21). Alukda D, Sturgis T, and Youan BBC (2011) Formulation of tenofovir-loaded functionalized solid lipid nanoparticles intended for HIV prevention. Journal of Pharmaceutical Sciences 100, 3345–3356. [PubMed: 21437910]

(22). Caron M, Besson G, Etenna SL-D, Mintsa-Ndong A, Mourtas S, Radaelli A, Morghen CDG, Loddo R, La Colla P, Antimisiaris SG, and Kazanji M (2010) Protective properties of non-nucleoside reverse transcriptase inhibitor (MC1220) incorporated into liposome against intravaginal challenge of Rhesus Macaques with RT-SHIV. Virology 405, 225–233. [PubMed: 20591460]

(23). Shah LK, and Amiji MM (2006) Intracellular delivery of saquinavir in biodegradable polymeric nanoparticles for HIV/AIDS. Pharm Res 23, 2638–45. [PubMed: 16969696]

(24). Jiang Y, Cao S, Bright DK, Bever AM, Blakney AK, Suydam IT, and Woodrow KA (2015) Nanoparticle-Based ARV Drug Combinations for Synergistic Inhibition of Cell-Free and Cell-Cell HIV Transmission. Mol Pharm 12, 4363–74. [PubMed: 26529558]

(25). Centers for Disease Control and Prevention: US Public Health Service. Preexposure prophylaxis for the prevention of HIV infection in the United States—2017 Update: a clinical practice guideline. https://www.cdc.gov/hiv/pdf/risk/prep/cdc-hiv-prep-guidelines-2017.pdf. Accessed on November 11, 2018.

(26). Tang EC, Vittinghoff E, Anderson PL, Cohen SE, Doblecki-Lewis S, Bacon O, Coleman ME, Buchbinder SP, Chege W, Kolber MA, Elion R, Shlipak M, and Liu AY (2018) Changes in Kidney Function Associated With Daily Tenofovir Disoproxil Fumarate/Emtricitabine for HIV Preexposure Prophylaxis Use in the United States Demonstration Project. J Acquir Immune Defic Syndr 77, 193–198. [PubMed: 28991887]

(27). Gandhi M, Glidden DV, Mayer K, Schechter M, Buchbinder S, Grinsztejn B, Hosek S, Casapia M, Guanira J, Bekker LG, Louie A, Horng H, Benet LZ, Liu A, and Grant RM (2016) Association of age, baseline kidney function, and medication exposure with declines in creatinine clearance on pre-exposure prophylaxis: an observational cohort study. The lancet. HIV 3, e521–e528. [PubMed: 27658870]

(28). Kasonde M, Niska RW, Rose C, Henderson FL, Segolodi TM, Turner K, Smith DK, Thigpen MC, and Paxton LA (2014) Bone mineral density changes among HIV-uninfected young adults in a randomised trial of pre-exposure prophylaxis with tenofovir-emtricitabine or placebo in Botswana. PLoS One 9, e90111.

(29). Mulligan K, Glidden DV, Anderson PL, Liu A, McMahan V, Gonzales P, Ramirez-Cardich ME, Namwongprom S, Chodacki P, de Mendonca LM, Wang F, Lama JR, Chariyalertsak S, Guanira JV, Buchbinder S, Bekker LG, Schechter M, Veloso VG, and Grant RM (2015) Effects of Emtricitabine/Tenofovir on Bone Mineral Density in HIV-Negative Persons in a Randomized, Double-Blind, Placebo-Controlled Trial. Clinical Infectious Diseases 61, 572–80. [PubMed: 25908682]

(30). Abdool Karim Q, Abdool Karim SS, Frohlich JA, Grobler AC, Baxter C, Mansoor LE, Kharsany AB, Sibeko S, Mlisana KP, Omar Z, Gengiah TN, Maarschalk S, Arulappan N, Mlotshwa M,

Morris L, and Taylor D (2010) Effectiveness and safety of tenofovir gel, an antiretroviral microbicide, for the prevention of HIV infection in women. Science 329, 1168–74. [PubMed: 20643915]

(31). Meng J, Agrahari V, Ezoulin MJ, Zhang C, Purohit SS, Molteni A, Dim D, Oyler NA, and Youan BC (2016) Tenofovir Containing Thiolated Chitosan Core/Shell Nanofibers: In Vitro and in Vivo Evaluations. Mol Pharm 13, 4129–4140. [PubMed: 27700124]

(32). Destache CJ, Mandal S, Yuan Z, Kang G, Date AA, Lu W, Shibata A, Pham R, Bruck P, Rezich M, Zhou Y, Vivekanandan R, Fletcher CV, and Li Q (2016) Topical Tenofovir Disoproxil Fumarate Nanoparticles Prevent HIV-1 Vaginal Transmission in a Humanized Mouse Model. Antimicrob Agents Chemother 60, 3633–9. [PubMed: 27044548]

(33). Endsley AN, and Ho RJY (2012) Enhanced anti-HIV efficacy of indinavir after inclusion in CD4-targeted lipid nanoparticles. J Acquir Immune Defic Syndr 61, 417–424. [PubMed: 22743598]

(34). Richman DD, Fischl MA, Grieco MH, Gottlieb MS, Volberding PA, Laskin OL, Leedom JM, Groopman JE, Mildvan D, and Hirsch MS (1987) The toxicity of azidothymidine (AZT) in the treatment of patients with AIDS and AIDS-related complex. N Engl J Med 317, 192–197. [PubMed: 3299090]

(35). Barry M, Howe J, Back D, Swart A, Breckenridge A, Weller I, Beeching N, and Nye F (1994) Zidovudine pharmacokinetics in zidovudine-induced bone marrow toxicity. Br J Clin Pharmacol 37, 7–12. [PubMed: 8148221]

(36). Joshy KS, Susan MA, Snigdha S, Nandakumar K, Laly AP, and Sabu T (2018) Encapsulation of zidovudine in PF-68 coated alginate conjugate nanoparticles for anti-HIV drug delivery. Int J Biol Macromol 107, 929–937. [PubMed: 28939525]

(37). Pedreiro LN, Stringhetti B, Cury F, and Gremiao MP (2016) Mucoadhesive Nanostructured Polyelectrolyte Complexes as Potential Carrier to Improve Zidovudine Permeability. J Nanosci Nanotechnol 16, 1248–56. [PubMed: 27433574]

(38). Dalpiaz A, Contado C, Mari L, Perrone D, Pavan B, Paganetto G, Hanuskova M, Vighi E, and Leo E (2014) Development and characterization of PLGA nanoparticles as delivery systems of a prodrug of zidovudine obtained by its conjugation with ursodeoxycholic acid. Drug Deliv 21, 221–32. [PubMed: 24134683]

(39). Mainardes RM, Gremiao MP, Brunetti IL, da Fonseca LM, and Khalil NM (2009) Zidovudine-loaded PLA and PLA-PEG blend nanoparticles: influence of polymer type on phagocytic uptake by polymorphonuclear cells. J Pharm Sci 98, 257–67. [PubMed: 18425813]

(40). Aykac A, Noiray M, Malanga M, Agostoni V, Casas-Solvas JM, Fenyvesi E, Gref R, and Vargas-Berenguel A (2017) A non-covalent “click chemistry” strategy to efficiently coat highly porous MOF nanoparticles with a stable polymeric shell. Biochim Biophys Acta Gen Subj 1861, 1606–1616. [PubMed: 28137620]

(41). Kedersha NL, and Rome LH (1986) Isolation and characterization of a novel ribonucleoprotein particle: large structures contain a single species of small RNA. J Cell Biol 103, 699–709. [PubMed: 2943744]

(42). Kedersha NL, Miquel MC, Bittner D, and Rome LH (1990) Vaults. II. Ribonucleoprotein structures are highly conserved among higher and lower eukaryotes. J Cell Biol 110, 895–901. [PubMed: 1691193]

(43). Kong LB, Siva AC, Rome LH, and Stewart PL (1999) Structure of the vault, a ubiquitous celular component. Structure 7, 371–9. [PubMed: 10196123]

(44). Tanaka H, Kato K, Yamashita E, Sumizawa T, Zhou Y, Yao M, Iwasaki K, Yoshimura M, and Tsukihara T (2009) The structure of rat liver vault at 3.5 angstrom resolution. Science 323, 384–8. [PubMed: 19150846]

(45). Kickhoefer VA, Siva AC, Kedersha NL, Inman EM, Ruland C, Streuli M, and Rome LH (1999) The 193-kD vault protein, VPARP, is a novel poly(ADP-ribose) polymerase. J Cell Biol 146, 917–28. [PubMed: 10477748]

(46). Kickhoefer VA, Liu Y, Kong LB, Snow BE, Stewart PL, Harrington L, and Rome LH (2001) The Telomerase/vault-associated protein TEP1 is required for vault RNA stability and its association with the vault particle. J Cell Biol 152, 157–64. [PubMed: 11149928]

(47). Kickhoefer VA, Stephen AG, Harrington L, Robinson MO, and Rome LH (1999) Vaults and telomerase share a common subunit, TEP1. J Biol Chem 274, 32712–7. [PubMed: 10551828]

(48). Buehler DC, Marsden MD, Shen S, Toso DB, Wu X, Loo JA, Zhou ZH, Kickhoefer VA, Wender PA, Zack JA, and Rome LH (2014) Bioengineered Vaults: Self-Assembling Protein Shell-Lipophilic Core Nanoparticles for Drug Delivery. ACS Nano 8, 7723–7732. [PubMed: 25061969]

(49). Kar UK, Srivastava MK, Andersson A, Baratelli F, Huang M, Kickhoefer VA, Dubinett SM, Rome LH, and Sharma S (2011) Novel CCL21-vault nanocapsule intratumoral delivery inhibits lung cancer growth. PLoS One 6, e18758.

(50). Benner NL, Zang X, Buehler DC, Kickhoefer VA, Rome ME, Rome LH, and Wender PA (2017) Vault nanoparticles: chemical modifications for imaging and enhanced delivery. ACS Nano 11, 872–881. [PubMed: 28029784]

(51). Kar UK, Jiang J, Champion CI, Salehi S, Srivastava M, Sharma S, Rabizadeh S, Niazi K, Kickhoefer V, Rome LH, and Kelly KA (2012) Vault nanocapsules as adjuvants favor cell-mediated over antibody-mediated immune responses following immunization of mice. PLoS One 7, e38553.

(52). Champion CI, Kickhoefer VA, Liu G, Moniz RJ, Freed AS, Bergmann LL, Vaccari D, Raval-Fernandes S, Chan AM, Rome LH, and Kelly KA (2009) A vault nanoparticle vaccine induces protective mucosal immunity. PLoS One 4, e5409.

(53). Kickhoefer VA, Garcia Y, Mikyas Y, Johansson E, Zhou JC, Raval-Fernandes S, Minoofar P, Zink JI, Dunn B, Stewart PL, and Rome LH (2005) Engineering of vault nanocapsules with enzymatic and fluorescent properties. Proc Natl Acad Sci U S A 102, 4348–52. [PubMed: 15753293]

(54). Wang M, Abad D, Kickhoefer VA, Rome LH, and Mahendra S (2015) Vault Nanoparticles Packaged with Enzymes as an Efficient Pollutant Biodegradation Technology. ACS Nano 9, 10931–40. [PubMed: 26493711]

(55). Kickhoefer VA, Han M, Raval-Fernandes S, Poderycki MJ, Moniz RJ, Vaccari D, Silvestry M, Stewart PL, Kelly KA, and Rome LH (2009) Targeting vault nanoparticles to specific cell surface receptors. ACS Nano 3, 27–36. [PubMed: 19206245]

(56). Zhu Y, Jiang J, Said-Sadier N, Boxx G, Champion C, Tetlow A, Kickhoefer VA, Rome LH, Ojcius DM, and Kelly KA (2015) Activation of the NLRP3 inflammasome by vault nanoparticles expressing a chlamydial epitope. Vaccine 33, 298–306. [PubMed: 25448112]

(57). Rome LH, and Kickhoefer VA (2013) Development of the vault particle as a platform technology. ACS Nano 7, 889–902. [PubMed: 23267674]

(58). Tadayoni BM, Friden PM, Walus LR, and Musso GF (1993) Synthesis, in vitro kinetics and in vivo studies on protein conjugates of AZT: evaluation as a transport system to increase brain delivery. Bioconjug Chem 4, 139–145. [PubMed: 7873646]

(59). Giammona G, Cavallaro G, Fontana G, Pitarresi G, and Carlisi B (1998) Coupling of the antiviral agent zidovudine to polyaspartamide and in vitro drug release studies. J Control Release 54, 321–331. [PubMed: 9766252]

(60). Wannachaiyasit S, Chanvorachote P, and Nimmannit U (2008) A novel anti-HIV dextrin–zidovudine conjugate improving the pharmacokinetics of zidovudine in rats. AAPS PharmSciTech 9, 840. [PubMed: 18626772]

(61). Ray AS, Fordyce MW, and Hitchcock MJM (2016) Tenofovir alafenamide: A novel prodrug of tenofovir for the treatment of Human Immunodeficiency Virus. Antiviral Res 125, 63–70. [PubMed: 26640223]

(62). Schoch J, Wiessler M, and Jäschke A (2010) Post-synthetic modification of DNA by inverse-electron-demand Diels− Alder reaction. J Am Chem Soc 132, 8846–8847. [PubMed: 20550120]

(63). Blackman ML, Royzen M, and Fox JM (2008) Tetrazine ligation: fast bioconjugation based on inverse-electron-demand Diels− Alder reactivity. J Am Chem Soc 130, 13518–13519. [PubMed: 18798613]

(64). Jain N, Smith SW, Ghone S, and Tomczuk B (2015) Current ADC linker chemistry. Pharm Res 32, 3526–3540. [PubMed: 25759187]

(65). King HD, Dubowchik GM, Mastalerz H, Willner D, Hofstead SJ, Firestone RA, Lasch SJ, and Trail PA (2002) Monoclonal antibody conjugates of doxorubicin prepared with branched peptide linkers: inhibition of aggregation by methoxytriethyleneglycol chains. J Med Chem 45, 4336–4343. [PubMed: 12213074]

(66). Hollander I, Kunz A, and Hamann PR (2007) Selection of reaction additives used in the preparation of monomeric antibody− calicheamicin conjugates. Bioconjug Chem 19, 358–361. [PubMed: 17994681]

(67). Zhao RY, Wilhelm SD, Audette C, Jones G, Leece BA, Lazar AC, Goldmacher VS, Singh R, Kovtun Y, and Widdison WC (2011) Synthesis and evaluation of hydrophilic linkers for antibody–maytansinoid conjugates. J Med Chem 54, 3606–3623. [PubMed: 21517041]

(68). Doronina SO, Mendelsohn BA, Bovee TD, Cerveny CG, Alley SC, Meyer DL, Oflazoglu E, Toki BE, Sanderson RJ, Zabinski RF, Wahl AF, and Senter PD (2006) Enhanced Activity of Monomethylauristatin F through Monoclonal Antibody Delivery: Effects of Linker Technology on Efficacy and Toxicity. Bioconjugate Chemistry 17, 114–124. [PubMed: 16417259]

(69). Stephen AG, Raval-Fernandes S, Huynh T, Torres M, Kickhoefer VA, and Rome LH (2001) Assembly of vault-like particles in insect cells expressing only the major vault protein. J Biol Chem 276, 23217–20. [PubMed: 11349122]

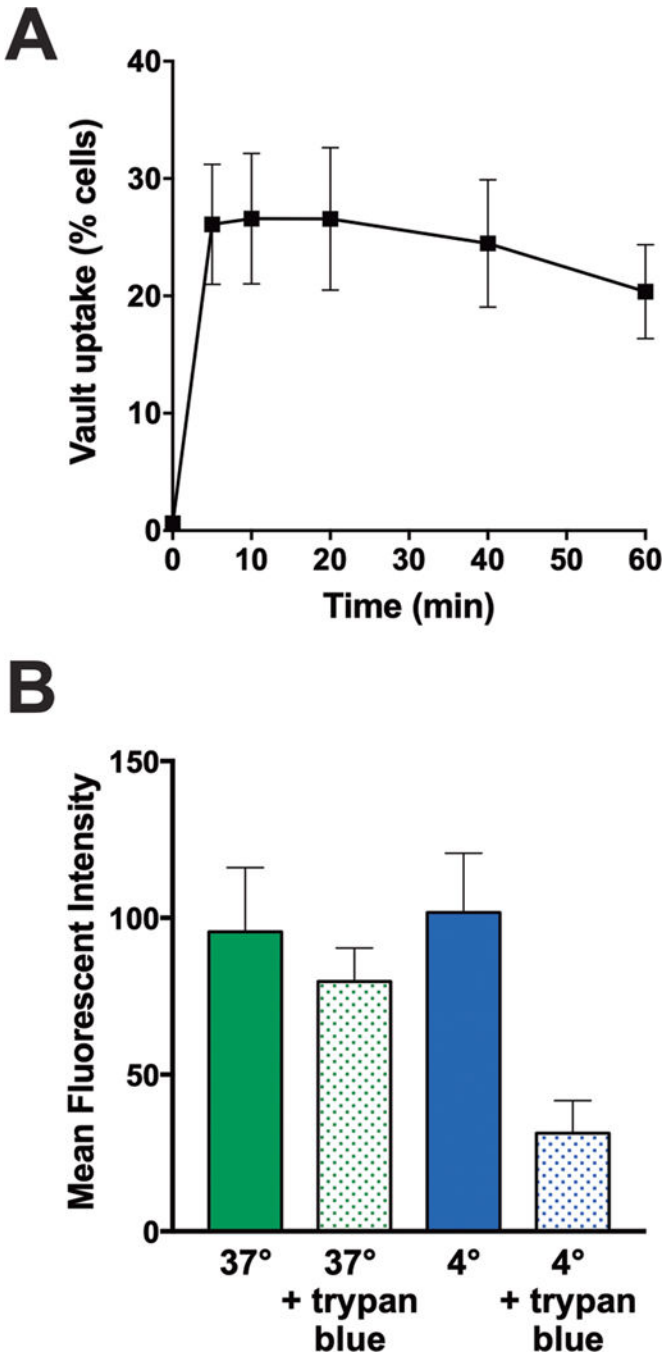

Figure 1. Vault internalization by human PBMC.

(A) Fluorescence-labeled vaults were incubated with human PBMC for the indicated times, and then cell association (as indicated by cell fluorescence) was quantified via flow cytometry. Maximal cell fluorescence was achieved by 20 minutes. Data shown are mean ± standard deviation of 3 independent experiments. **(B)** To assess whether cell association occurs via surface binding versus internalization, PBMC were incubated with fluorescence-labeled vaults at 37°C and 4°C in the presence and absence of the extracellular fluorescence quencher trypan blue. At 37°C trypan blue did not significantly quench fluorescence,

suggesting vault internalization, whereas at 4°C (inhibiting internalization) trypan blue decreased fluorescence. Data shown as mean ± standard deviation of 4 independent experiments.

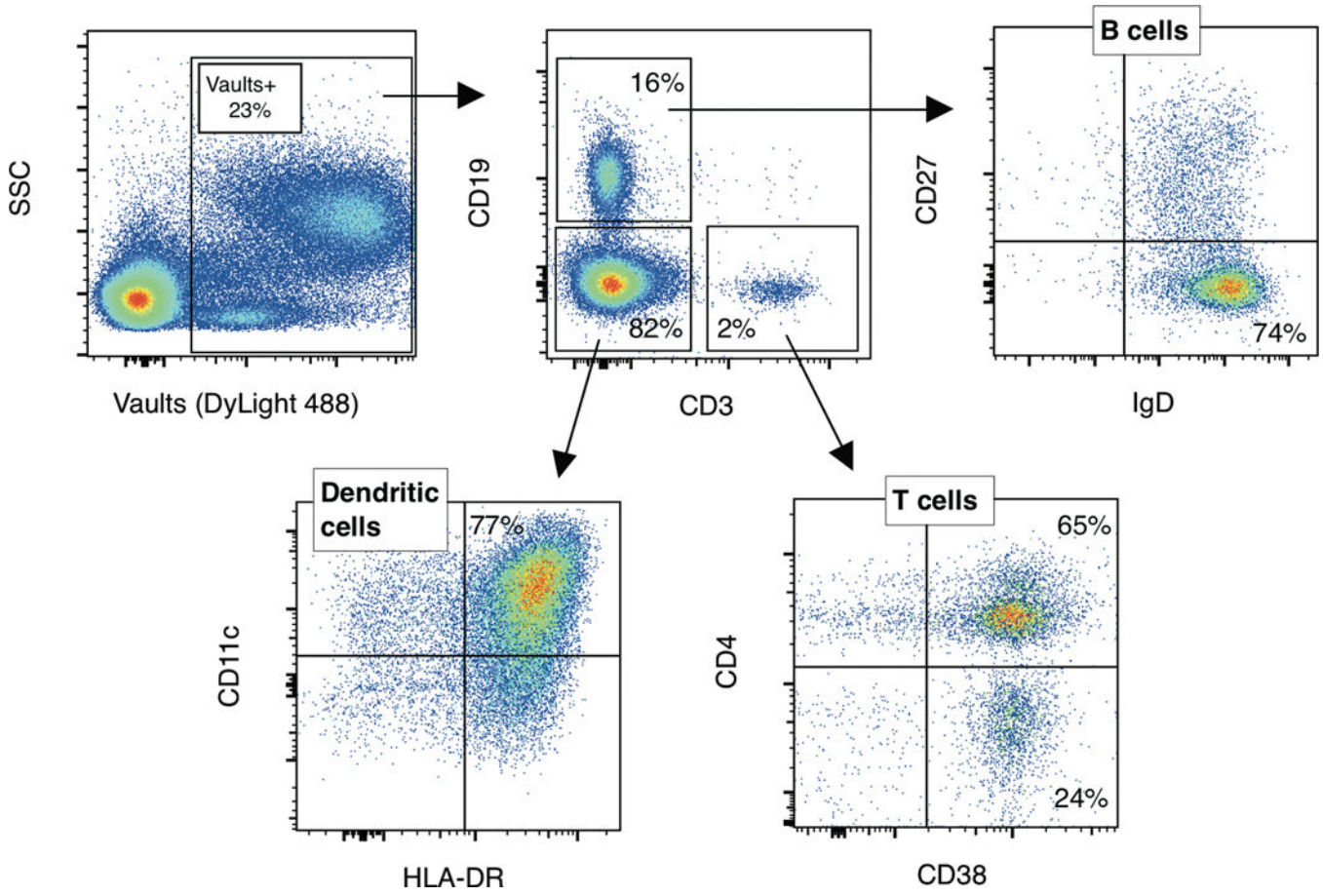

Figure 2. Definition of PBMC subsets that internalize recombinant vaults.

Human PBMC were incubated with fluorescence-labeled recombinant vaults and then stained with fluorescence-conjugated antibodies to identify specific cellular subsets using flow cytometry. Approximately 23% of all PBMC internalized vaults, as shown in the top left panel. Of these, approximately 16% were B cells ($CD19^+$), 2% were T cells ($CD3^+$) and 82% were not B or T cells. This latter subset was comprised primarily (77%) of dendritic cells ($CD11c^+HLA\text{-}DR^+$, bottom left). Among B cells that internalized vaults, the majority (74%) were naïve B cells ($CD27^-IgD^+$, top right). Among T cells that internalized vaults, the majority (65%) were activated $CD4^+$ T cells (bottom right).

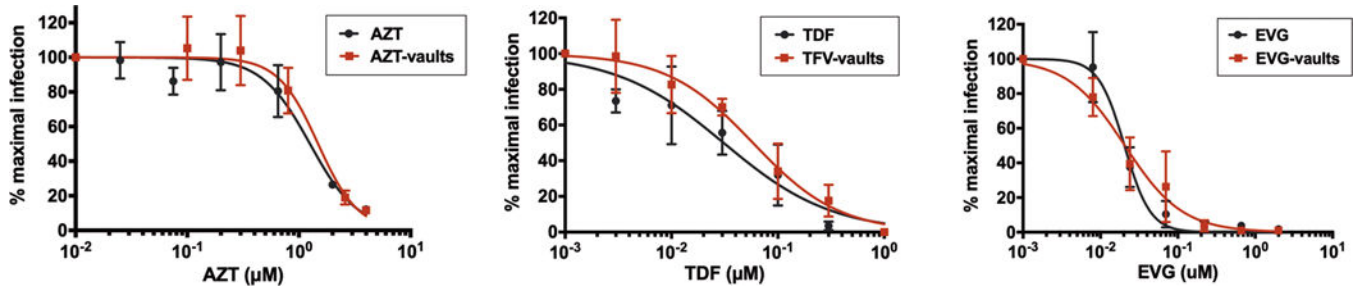

Figure 3. Vault-conjugated antiretroviral drugs inhibit HIV-1 infection in human PBMC.

Equivalent concentrations of vault-conjugated drug or free drug were added to PBMC prior to infection with HIV-1 for 2 hours. Infection was quantified by intracellular p24 staining and normalized to no drug condition. Data shown as mean ± standard deviation for 3 independent experiments.

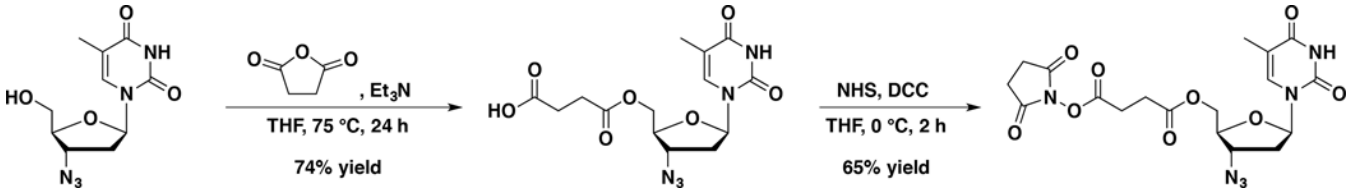

Scheme 1.
Synthesis of AZT-NHS.

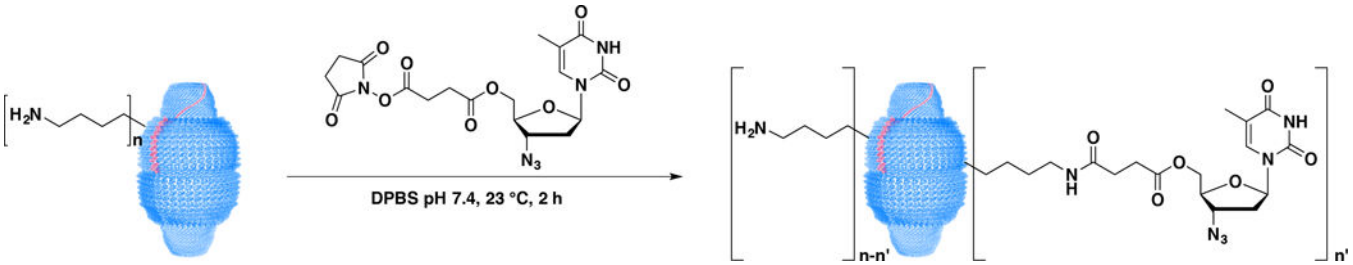

Scheme 2.
Conjugation of AZT-NHS to recombinant vaults.

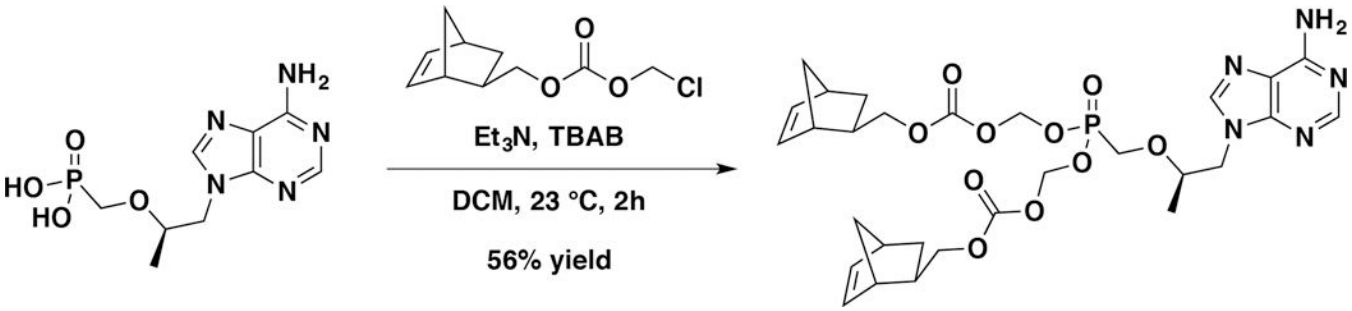

Scheme 3.
Synthesis of TFV-Nor.

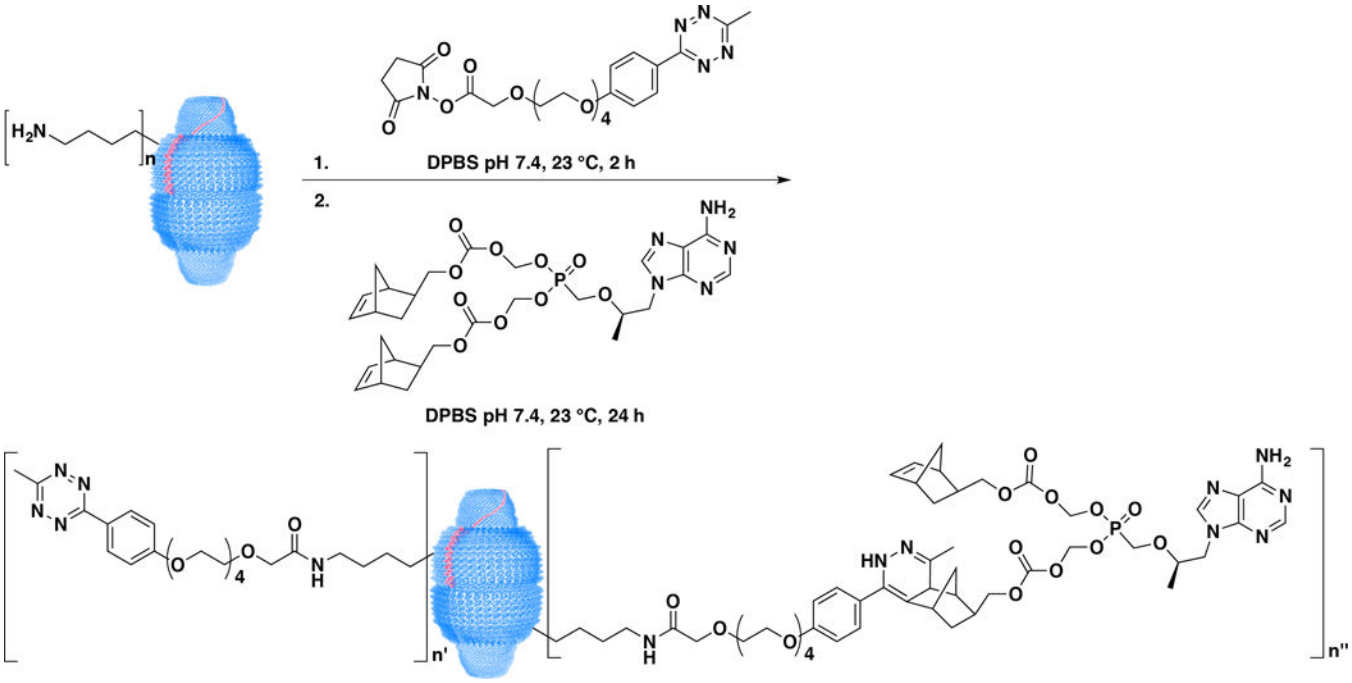

Scheme 4.
Conjugation of TFV-Nor to vaults.

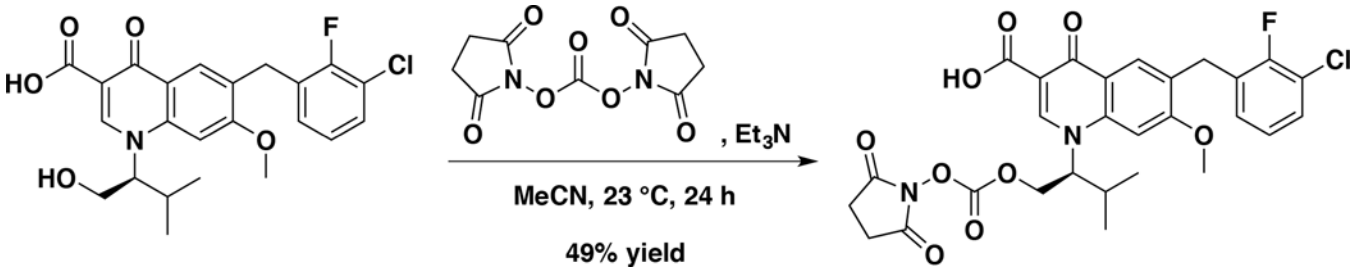

Scheme 5.
Synthesis of EVG-NHS.

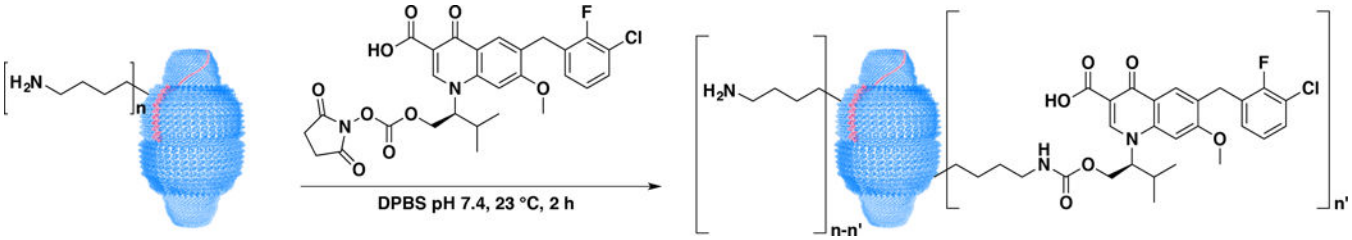

Scheme 6.
Conjugation of EVG-NHS to vaults.

Table 1.

Efficiency of antiretroviral drug conjugation to vaults

Drug	Equivalents/Lysine	# Drugs/Vault	% Derivatization
Zidovudine	3.28	1296 ± 3.19	37.8
Tenofovir	2.25 (linker)/ 5 (drug)	640 ± 3.74	18.8
Elvitegravir	0.3	67 ± 4.81	1.9